Applied Surface Science 336 (2015) 129–132

Contents lists available at ScienceDirect

Applied Surface Science

journal homepage: www.elsevier.com/locate/apsusc

Ar ions irradiation effects in ZrN thin films grown by pulsed laser deposition

D. Craciun[a], G. Socol[a], G. Dorcioman[a], D. Simeone[b], D. Gosset[b], S. Behdad[c], B. Boesl[c], V. Craciun[a,*]

[a] Laser Department, National Institute for Laser, Plasma, and Radiation Physics, Bucharest-Magurele, Romania
[b] CEA/DEN/DANS/DM2S/SERMA/LEPP-LRC CARMEN CEN Saclay France & CNRS/SPMS UMR8785 LRC CARMEN, Ecole Centrale de Paris, F92292 Chatenay Malabry, France
[c] Department of Mechanical and Materials Engineering, Florida International University, Miami, FL 33174, USA

ARTICLE INFO

Article history:
Received 9 July 2014
Received in revised form 7 October 2014
Accepted 8 October 2014
Available online 18 October 2014

Keywords:
ZrN
Hard coating
Pulsed laser deposition
Radiation effects

ABSTRACT

Thin ZrN films (<500 nm) were grown on (1 0 0)Si substrates at a substrate temperature of 500 °C by the pulsed laser deposition (PLD) technique using a KrF excimer laser under CH_4 or N_2 atmosphere. Glancing incidence X-ray diffraction showed that films were nanocrystalline, while X-ray reflectivity studies indicated that the films were very dense and with a smooth surface. The films were used to study the effect of 800 keV Ar ion irradiation on their structure and properties. After irradiation with a dose of 10^{14} at/cm^2 the lattice parameter and crystallites size did marginally change. However, after irradiation with a 10^{15} at/cm^2 dose, a clear increase in the lattice parameter accompanied by a significant decrease in nanohardness and Young modulus were observed.

1. Introduction

Zirconium nitride, ZrN, possesses both ceramic and metallic characteristics: very high melting point [1], high hardness (30–35 GPa) [2,3], good wear resistance [4], high thermochemical stability [5], low electrical resistivity [6], and good biocompatibility [7]. In addition, because of its low cross section capture for neutrons it could be used as a protective coating for nuclear application. Several techniques have been employed to obtain high quality ZrN thin films to investigate their properties [2–8]. Pulsed laser deposition (PLD) technique is very suitable for such studies, since by controlling the laser irradiation parameters and deposition conditions films with various structural qualities and Zr/N values could be obtained [3,9,10]. Moreover, such films could be deposited at moderate substrate temperatures, below 550 °C [9,10]. We showed previously that such PLD grown ZrN films exhibited high hardness and Young modulus values and low friction coefficients and wear rates [10].

The effect of Ar ion irradiation on films has been studied since it is able to qualitatively described disorder induced by neutron irradiation at the micrometer-scale. On the atomic level, on the other hand, the main interest of irradiation lies in the fact that many defects can be created without modifying the chemistry of the material. This work tries to qualitatively estimate the impact of radiation damages produced in nuclear plants in this materials, a potential candidate for liners of IV generation nuclear plants. It is focused on the investigation of structural and mechanical properties of such thin films combining several investigations techniques in order to understand the link between structural damage caused by irradiation and mechanical properties in ceramics films.

2. Experimental details

The PLD experimental set up used to deposit the films has been previously described [9,10]. A KrF excimer laser (λ = 248 nm, pulse duration τ = 25 ns, 8 J/cm^2 fluence, 40 Hz repetition rate) is used to ablate a ZrN target in a stainless steel chamber. The films were deposited on p^{++} (1 0 0)Si substrates (MEMC Electronic Materials, Inc.) at a nominal substrate temperature of 500 °C under a high purity atmosphere of CH_4 or N_2. Previous results indicated that a low gas pressure during deposition had a beneficial effect on the structure of the deposited films. CH_4 was also used besides N_2 since the incorporation of small amounts of C in the ZrN lattice resulted in slightly better mechanical properties [10]. The deposition conditions are displayed in Table 1.

* Corresponding author. Tel.: +40 212303378.
E-mail address: valentin.craciun@inflpr.ro (V. Craciun).

http://dx.doi.org/10.1016/j.apsusc.2014.10.032
0169-4332/

Table 1
Deposition conditions and structural properties of the deposited films.

Sample	Atmosphere (Pa)	Number of pulses	Lattice parameter (Å)		Density (g/cm^3)		Surface roughness, RMS (Å)	Grain size (Å)	Micro-strain (%)
			XRD	GIXRD	XRR	GIXRD	XRR/AFM	W-H	W-H
ZrN1	2×10^{-3} CH_4	20,000	4.684	4.543	7.09	7.406	6/4	110	0.9
ZrN3	2×10^{-3} N_2	20,000	4.667	4.546	7.05	7.387	7/5	155	1.3

The deposited ZrN films were irradiated at room temperature by 800 keV Ar ions at a flux of 10^{11} cm^{-2} s^{-1}. The kinetic energy of Ar ions was chosen to maximize the nuclear energy loss inside the ZrN layer, the electronic energy loss being one order of magnitude smaller than the nuclear energy loss. The displacement per atom (dpa) value was calculated from SRIM integrating all displacements induced by atomic collision between Ar atoms and zirconium and nitrogen but also collisions between nitrogen and zirconium atoms with atoms at rest in the crystal. As pointed out by the SRIM simulations, atomic mixing occurred at the ZrN/Si interface. However, the characteristic length of this mixing calculated from the Si penetration into the ZrN layer remained smaller than five nanometers. The amount of Si in the ZrN layer was equal to 0.04 atomic fraction for the highest fluence used here (10^{15} cm^{-2}). Both the mixing length as well as the atomic concentration remained relatively small and did not play an important part in XRD and reflectivity measurements.

For all studied samples, the displacement rate was equal to 4.6 10^{-4} dpa/s. Two distinct irradiations were performed at 4.6 dpa and 46 dpa (with fluences of 10^{14} and 10^{15} cm^{-2}) in order study the impact of radiation damages on the structure and mechanical properties of ZrN thin films. The temperature during irradiation was monitored by a thermocouple stuck on the back of the sample avoiding radiation damages on it. No important variation of the temperature was measured during irradiations, suggesting that the temperature increasing was smaller than 50 K for all performed irradiations. To study the structural evolution (unit cell parameters, space group evolution) and microstructural evolution (sizes of Coherent Diffracting Domains, CDD, micro strain induced by radiation damages), glancing incidence X-ray diffraction (GIXRD) investigations were performed on the films. The use of the GIXRD technique to collect diffraction patterns from thin films was described in details in previuos works [11,12] and successfully applied to study radiation damage in irradiated materials [13,14]. Whithin the glancing incidence technique, diffraction patterns are collected from crystallites that have the planes tilted at a certain angle with respect to the surface normal.

From calculations of the X-ray beam penetration depth versus the incidence angle a value of 1°, which gives an X-ray penetration depth of 400 nm inside the ZrC sample, was selected for the incidence angle for all measurements. This value was choosen for a twofold reason. First of all, it is associated with the maximum of damage peak in the material as pointed out in Fig. 3. On the other hand, we assumed that mechanical or chemical effects due to lattice misfit between the Si(1 0 0) wafer and the ZrN film were negligible.

The films mass density, thickness, and surface roughness were obtained from simulations of the XRR curves using a commercially available model (X'Pert Reflectivity) consisting of three layers: interfacial layer, accounting for the silicon native oxide and any ions that were subplanted/mixed within this layer [8,15,16], the deposited nitride layer and a surface contamination layer accounting for the hydroxide/carbon layer present at the topmost surface when films were exposed to the ambient. Atomic force microscopy (AFM) and scanning electron microscopy (SEM) were also used to investigate the surface morphology of the deposited samples.

The mechanical properties of the thin films were investigated using a Hysitron TI900 Triboindenter with a 100 nm diamond Berkovich tip. Tip area calibration was performed on a standard fused silica sample before the test. The indentation experiments were performed in quasi-static indentation mode, with maximum load of 1000 μN. A 4 × 4 array of 16 indents, 5 μm apart from each other was done on each sample. The loading, hold, and unloading times were 10, 3, and 10 s respectively. To minimize substrate contributions, the hardness and reduced modulus were determined from load-displacement contact depths between 30 and 50 nm following the model of Oliver and Pharr [17].

3. Results and discussion

According to GIXRD and XRR results, which are included in Table 1, the deposited films were nanocrystalline, dense and with a low surface roughness [9]. Symmetrical XRD scans showed that films were slightly (1 1 1) textured, a typical texture for rock-salt type structures, where (1 1 1) planes have the highest atomic density. Williamson–Hall plots were used to estimate the crystallite sizes and micro-strain values [10], which are also displayed in Table 1. The rather large values estimated for the micro-strain were caused by defects induced by energetic ions and atoms from the plasma that bombarded the growing film during deposition [8,15,16]. The difference between the lattice parameter values extracted from symmetrical scans (out of plane) versus those extracted from GIXRD scans (in plane) was caused by the presence of a compressive stress in the deposited films [8–10].

The density estimated from XRR simulations was significantly lower than that estimated from GIXRD results, which correspond to fully stoichiometric compounds. First of all, since the films were under compressive stress the in plane lattice parameter was larger than the out of plane parameter (see Table 2). Secondly, this suggests that the as-deposited films already contain vacancies. The very smooth surface of the deposited films indicated by the results of XRR curves simulations was confirmed by the AFM and SEM investigations, as shown in Figs. 1 and 2. The very dense structure and small crystallite size is also evident in the SEM image of a cross section of a fractured ZrN film.

In order to simulate radiation damages induced by 800 keV Ar ions in the ZrN thin layer, the penetration depth of Ar impinging ions as well as the number of Zr and N vacancies created in two distinct sub lattices were calculated within the binary collision framework (STRIM code) and displayed in Fig. 3. The displacement threshold energies were equal to 25 and 28 eV for Zr and N sub lattices in all simulations. The sputtering yield was equal to 0.7 and 1.6 at/ion for Zr and N sublattices. This implies that the sputtering occurring at the ZrN surface was equal to 0.1 and 1.6 nanometers for each sublattice for the most irradiated sample associated with a fluence of 10^{15} cm^{-2}, which is negligible and does not induced craters, able to increase drastically the roughness of the ZrN surface and then the slope of reflectivity curves after irradiation.

The nature and the energy of the impinging atoms ions were selected to obtain profiles of vacancies produced in two sub lattices that are relatively uniform along the thickness of the film as shown in Fig. 3. Such a distribution of vacancies ensures the avoidance of any spurious effects due to a damage gradient. On the other hand, we have calculated the atomic fraction of Ar ions implanted in the thin film, which is also plotted in Fig. 3 (green curve). This

Table 2
Lattice and microstructural parameters of the irradiated ZrN samples.

Sample	Ion fluen. (10^{14} cm^2)	a (Å)	Grain size (Å)	Micro-strain (%)	XRR-density (g/cm^3)	Dens. var. (%)
ZrN-1	1	4.544	92	0.8	6.88	2.8
ZrN-3	10	4.555	120	0.7	6.90	2.7

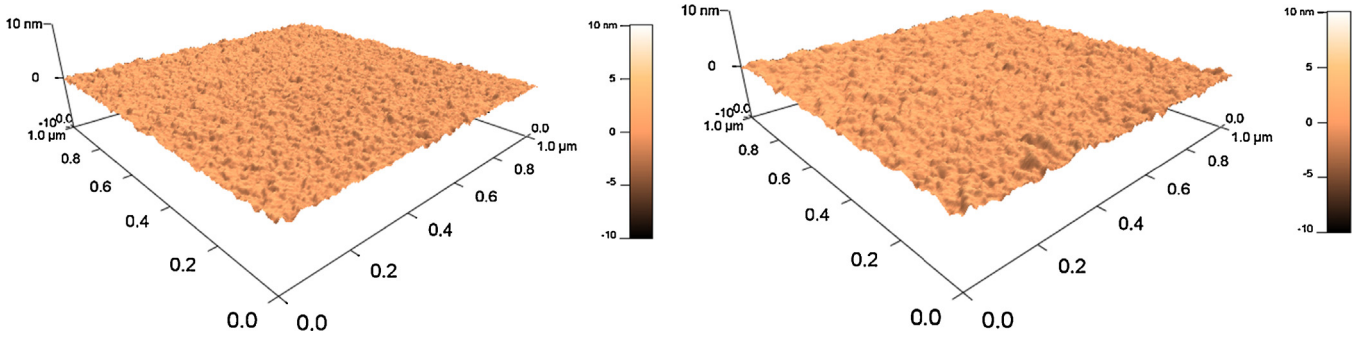

Fig. 1. AFM images of the surface morphology of ZrN1 (left) and ZrN3 (right) as-deposited films.

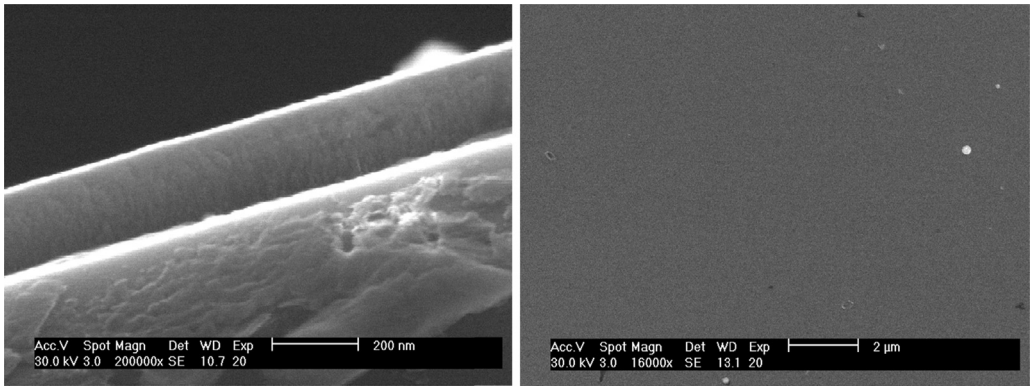

Fig. 2. SEM images of a fractured ZrN film and its surface.

atomic fraction is peaked near the substrate-film interface and remains lower than 5%. We therefore assumed that this concentration was small and did not significantly affect the mechanical properties of the film. In order to quantify the radiation damage induced by 800 keV Ar ions inside the thin film, the displacement cross section was also computed. From the analysis of SRIM simulations plotted in Fig. 3, this displacement cross section was equal to 4.6×10^{-15} cm^{-2}.

Fig. 4 displays the diffraction patterns collected on two ZrN irradiated samples. The diffraction patterns collected from the as

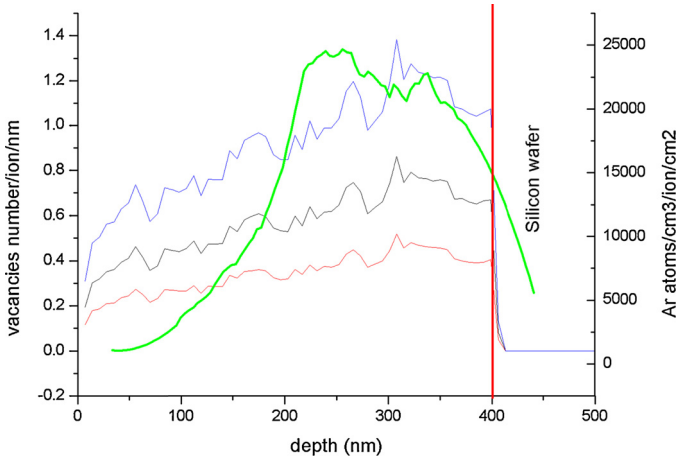

Fig. 3. SRIM calculations of the amount of Zr and N vacancies (red and black line, respectively; blue line indicates the total number of vacancies) created into Zr and N lattices as a function of the depth for 800 keV Ar ion irradiation. Atomic fraction of Ar ions implanted in the thin film is also plotted by the green curve. (For interpretation of the references to color in this figure legend, the reader is referred to the web version of this article.)

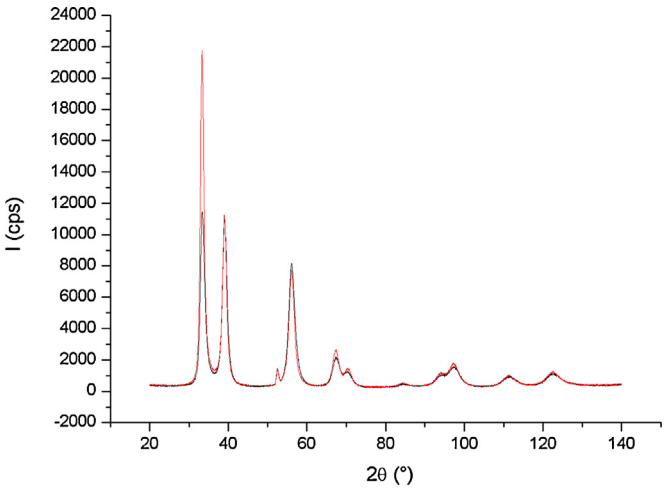

Fig. 4. Comparison between the diffraction patterns collected on ZrN samples irradiated at two distinct fluences (black 10^{14} cm^2; red: 10^{15} cm^2) under an incidence angle of 1°. (For interpretation of the references to color in this figure legend, the reader is referred to the web version of this article.)

Table 3
Nanoindentation results for as-deposited and irradiated ZrN films.

Sample	Irradiation (at/cm^2)	E (GPa)		H (GPa)	
		As-deposited	After irradiation	As-deposited	After irradiation
ZrN1	10^{14}	245	161	32.5	16.2
ZrN3	10^{15}	255	162	34.5	15.4

deposited samples were not plotted for clarity. All peaks corresponding to the rock-salt lattice of ZrN [18] were present. The small peak located at around $2\theta \sim 53^\circ$ was caused by the Si substrate. CDDs appeared to be anisotropic, flattened along the (1 1 1) directions. After irradiation with a dose of 10^{14} ions/cm^2, the change in lattice parameters is rather small, almost at the resolution limit. However, the higher ion fluence of 10^{15} ions/cm^2 caused a clear increase in the lattice parameter of the film. Both doses caused a decrease of the microstrain present in the films, more so for the ZrN_3 sample, that also had a higher initial value. The causes for rather sudden large structural changes after the higher irradiation dose remained so far unclear. ZrN behaves like a metal and T_{irr} (300 K)/$T_{melting}$ (3225 K) is less than 0.1. This ratio is too small to indicate any diffusion of point defects (vacancies and interstitials) and the production of precipitates, voids or dislocation loops. The observed increase of the lattice parameter for thin ZrN films irradiated is in line with the report of Janse van Vuuren et al. [19] but quite different from the report of Lu et al. [20], where a structural contraction after irradiation with Ne ions was measured. Such observations underline the importance of such studies, where the crystallites size and stress levels could influence the change of the lattice parameters.

The results of nanoindentation measurements, hardness and Young modulus, are displayed in Table 3. AFM investigations of the nanoindentation sites showed no measurable pile-up or distortions of the symmetrical shape, factors that could affect the accuracy of the measurements for such thin films and low indentation depths. It appears that both irradiation conditions greatly affects the mechanical properties of the deposited films, more so for the higher irradiation dose. Although the reduction is significant it should be noticed that after the irradiation the films remained nevertheless hard and elastic. These reported results are quite different from those observed earlier [21], when irradiated ZrN films exhibited an increase of the hardness values from the low 20 GPa to more than 30 GPa, while the Young modulus was not significantly affected. The very high hardness values measured for our as-deposited ZrN films were explained by the small crystallite size, which does not allow for the presence of dislocations and the dense structure, which makes the sliding and rotation of crystallites very difficult [10]. After irradiation, the density decreased, which could account for easier movement of crystallites and explain the rather significant decrease in hardness values. Again, initial properties of the deposited ZrN seem to be critical for their behavior under ion irradiation.

4. Conclusions

Dense, polycrystalline and smooth films of ZrN were grown using the PLD technique under CH_4 or N_2 atmosphere. The effect of Ar ion irradiation on the structural and mechanical properties of these films was investigated. ZrN films irradiated with a dose of 10^{14} Ar ions/cm^2 did not show major structural changes, although their hardness was significantly lower than that measured for as-deposited films. After an irradiation with a dose of 10^{15} Ar ions/cm^2, significant structural changes consisting of a larger lattice parameter were observed, together with lower hardness and Young modulus values. These results showed that PLD grown ZrN films are suitable for the investigations of radiation effects on materials, especially since the stoichiometry, stress level and crystallite sizes greatly influence the behavior of films under irradiation. Further experiments to help understanding the causes of the increase of the lattice parameter and hardness decrease with high irradiation doses are underway.

Acknowledgements

This work was supported by grants of the Romanian Ministry of Education, ROSA STAR project number 60, CNCS – UEFISCDI, project number PN-II-RU-PD-2012-3–0346, and IFA-CEA C3-03. S.B. would like to thank the financial support from Florida International University Doctoral Evidence Acquisition Fellowship. The authors also acknowledge the help of N. Nabillon and N. Moncoffre of the team ACE of the CNRS/IPNL for having performed the Ar ion irradiations.

References

[1] W. Lengauer, Transition metal carbides, nitrides and carbonitrides, in: R. Riedel (Ed.), Handbook of Ceramic Hard Materials, vol. 1, Wiley-VCH, Weinheim, 2000.
[2] D. Martinez-Martinez, C. Lopez-Cartes, A. Fernandez, J.C. Sanchez-Lopez, Appl. Surf. Sci. 276 (2013) 121–126.
[3] H. Spillmann, P.R. Willmott, M. Morstein, P.J. Uggowitzer, Appl. Phys. A 73 (2001) 441–450.
[4] E. Silva, M.R. Figueiredo, R. Franz, R.E. Galindo, C. Palacio, A. Espinosa, S.V. Calderon, C. Mitterer, S. Carvalho, Surf. Coat. Technol. 205 (2010) 2134–2141.
[5] F.-H. Lu, W.-Z. Lo, Degradation of ZrN films at high temperature under controlled atmosphere, J. Vac. Sci. Technol. A 22 (2004) 2071.
[6] M. Del Re, R. Gouttebaron, J.-P. Dauchot, P. Leclere, G. Terwagne, M. Hecq, Surf. Coat. Technol. 174–175 (2003) 240–245.
[7] Y.C. Xin, C.L. Liu, K.F. Huo, G.Y. Tang, X.B. Tian, P.K. Chu, Surf. Coat. Technol. 203 (2009) 2554–2557.
[8] L.E. Koutsokeras, G. Abadias, J. Appl. Phys. 111 (2012) 093509.
[9] D. Craciun, G. Socol, N. Stefan, G. Dorcioman, M. Hanna, C.R. Taylor, E. Lambers, V. Craciun, Appl. Surf. Sci. 302 (May) (2014) 124–12813.
[10] G. Dorcioman, G. Socol, D. Craciun, N. Argibay, E. Lambers, M. Hanna, C.R. Taylor, V. Craciun, Appl. Surf. Sci. 306 (2014) 33–36.
[11] D. Simeone, G. Baldinozzi, D. Gosset, S. Lecaer, J.F. Berar, Thin Solid Films 530 (2013) 9–13.
[12] D. Simeone, G. Baldinozzi, D. Gosset, G. Zalczer, J.F. Berar, J. Appl. Crystallogr. 44 (2011) 1205–1210.
[13] D. Gosset, M. Dolle, D. Simeone, et al., Nucl. Instrum. Meth. Phys. Res. B 266 (12–13) (2008) 2801.
[14] D. Gosset, M. Dolle, D. Simeone, et al., J. Nucl. Mater. 373 (1–3) (2008) 123.
[15] F.M. D'Heurle, Metall. Trans. 1 (1970) 725–732.
[16] A. Perea, J. Gonzalo, C. Budtz-Jorgensen, G. Epurescu, J. Siegel, C.N. Afonso, J. Garcia-Lopez, J. Appl. Phys. 104 (2008) (Article No.: 084912).
[17] W.C. Oliver, G.M. Pharr, J. Mater. Res. 47 (1992) 1564.
[18] JCPDS – International Center for Diffraction Data, Copyright © JCPDS-ICDD 1996, card 35-0753.
[19] A. Janse van Vuuren, V.A. Skuratov, V.V. Uglov, J.H. Neethling, S.V. Zlotski, J. Nucl. Mater. 442 (November (1–3)) (2013) 507–511.
[20] F. Lu, M. Huang, F. Yaqoob, M. Lang, F. Namavar, C. Trautmann, H.T. Sun, R.C. Ewing, J. Lian, Appl. Phys. Lett. 101 (2012) (Article No.: 041904).
[21] G.W. Egeland, J.A. Valdez, S.A. Maloy, K.J. McClellan, K.E. Sickafus, G.M. Bond, J. Nucl. Mater. 435 (2013) 77–87.